DESIGN AND ANALYSIS OF A GRIPPING EFFECTOR MANUFACTURED USING ADDITIVE TECHNOLOGY

JOZEF TKAC[1], PETR BARON[1], DOMINIK TUPTA[2]

[1]Technical University of Kosice, Faculty of Manufacturing Technologies with a seat in Presov, Department of Computer Aided Manufacturing Technologies Presov, Slovakia

[2]Premy s.r.o., Slanska 70, Presov, Slovakia

DOI: 10.17973/MMSJ.2025_09_2025023

jozef.tkac@tuke.sk

The article deals with the design and implementation of a "compliant" gripping effector using additive FDM technology. It focuses on the possibilities of using flexible mechanisms that work on the principle of bending deformation instead of classic joints. As part of the solution, two effector prototypes were designed, made of PLA and PET-G materials, which were subsequently tested in terms of applied force, tension, and durability under cyclic loading. Ansys software was used to analyze mechanical behavior, which confirmed the more advantageous properties of PET-G, especially lower stress concentration and higher fatigue resistance. The output of the article is an effector with easy assembly, modular design, and the ability to quickly replace parts. The control was implemented using an Arduino programmable board. The results point to the practical potential of "compliant" mechanisms in the field of robotics, where flexibility, low weight, and rapid design adaptation are required.

KEYWORDS

Compliant mechanism, additive technologies, gripper, ansys, materials

1 INTRODUCTION

A mechanism is a mechanical device that is used to transmit force, energy, or motion. However, a "compliant" mechanism is a monolithic device that operates on the principles of elastic continuum to transmit the required force and motion. No mechanical components such as springs, screws, etc. are used in the construction of these mechanisms. In practice, it is possible to transform classical rigid mechanisms into "compliant" mechanisms using knowledge of pseudo-rigid bodies. Design is currently simplified using computer analysis, with "compliant" mechanisms meeting all requirements and taking advantage of all the benefits of these mechanisms. The authors of one of the articles developed a trimodal gripper for waste sorting that combines Nano PU adhesion, vacuum suction, and claws. Thanks to a visual system that does not use deep learning, the effector can quickly analyze objects and choose the optimal way to grasp them. Testing on 33 objects yielded a success rate of almost 97% [Sadeghian 2022].

The performance characteristics of Bernoulli grippers were investigated by the authors of the article [Mykhailyshyn 2022], who analyzed the influence of various parameters such as the method and shape of the compressed air supply. Simulation results showed that horizontal intake provides higher efficiency than vertical intake. The design and testing of a flexible finger as a component of a biomechanical hand for robotic and rehabilitation purposes was investigated by the authors in the article [Stojiljkovic 2023]. Two 3D printed prototypes were created and analyzed using FEA, manual measurements, and computer vision. The result was a validated model of a flexible finger, ready for practical use. The research study [Sun 2020] describes the development of a FEM framework for modeling bio-inspired flexible mechanisms for medical applications. Nonlinear solutions in the MATLAB environment allow the simulation of large deformations, tensile cables, and contact interactions. The accuracy of the model was verified using real-world tests of 3D printed prototypes. A Bernoulli gripper with an anti-vibration insert designed for handling textile materials was investigated in the literature [Mykhailyshyn 2023, Saga 2019]. The theoretical model takes into account the porosity of the material and its output is recommendations for geometry optimization. Experiments have confirmed reliable performance when handling breathable textiles. Another designed robotic gripper was powered by nitinol wires with shape memory. Three kinematic variants were proposed, whereas the most suitable configuration being analyzed mathematically and using simulations. The result is a compact, quiet, gearless solution suitable for industrial conditions [Kelemen 2022].

The design of a compact mechanism with high load capacity, large working space and good drive stability resulted in a systematic design procedure, through which they synthesized new mechanism configurations and verified their correctness using degrees of freedom analysis and the finite element method [Li 2021]. The article [Vishnu 2022] focuses on the experimental determination of key parameters for the design of a robotic end effector for strawberry picking, specifically the force required to grip a strawberry stalk. Research has shown that a safe gripping force that does not deform the stem is approximately 10 N. This force allows the manipulation of a strawberry weighing up to 50 grams even at an acceleration of the manipulator of up to 50 m/s^2. A force of 15 N is sufficient to cut a stem using a blade with a 16.6° bevel at an angle of 30°. This knowledge serves as design criteria for the development of efficient and environmentally friendly collection devices. The issue of accuracy of 3D printing nozzles for Bernoulli grippers was addressed in [Mykhailyshyn 2022]. The causes of geometry changes after production were identified and a methodology for calculating correction coefficients was proposed. The results confirmed that the best results are provided by nozzles printed with a layer of 0.05 mm. The article [Wang 2024] presents the design and testing of a robotic arm with a parallel gripper for crop harvesting. Inspired by bionics and optimized using simulations, it achieved a 23% reduction in harvesting losses compared to manual harvesting, and was validated on various fruit shapes and sizes. A review study [Elfferich 2022] analyzed 78 soft grippers designed for harvesting and handling agricultural crops. Grippers were divided into 13 technology categories and their performance was evaluated. The study highlights the need for standardization of testing and further development for specific applications.

In practice, it is possible to transform classical rigid mechanisms into "compliant" mechanisms using knowledge of pseudo-rigid bodies. Design is currently simplified using computer analysis, and "compliant" mechanisms will meet all the requirements and will take all the advantages of these mechanisms, such as:

- “Compliant” mechanisms consist of fewer parts. Individual parts can be manufactured by pressing, firing, additive manufacturing as a monolithic piece. In the mechanism manufacturing process, the advantages include reducing assembly time and complexity.
- With fewer parts, the weight of the mechanism is reduced, which makes these mechanisms a great asset in designs where weight reduction is necessary.

- The mechanisms do not need to be lubricated, they do not produce noise or vibrations.
- Since mechanisms achieve some of their mobility by deflecting a flexible member, it is possible to store energy in this member, which can then be released.
- Possibilities of downsizing structures. In practice, we call these downsized mechanisms MEMS [Zhang 2020, Tkac 2022].

The figure below shows the difference between the classic mechanism Fig. 1 b) and the "compliant" mechanism Fig. 1 a).

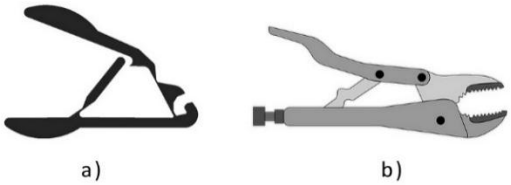

Figure 1. Example of a compliant (a) and classic (b) mechanism

A gripping effector is the end member of a robotic mechanism. It can be compared to the human hand, which allows us to lift any object and move it to another location. Robot grippers have wide applications in industry, but also in dangerous tasks in the military. The significant importance of gripping effectors can also be found in works requiring fine motor skills, such as medicine, but also in the production of microelectronic mechanisms [Zhang 2020, Tkac 2022].

Gripping effectors can be divided from several aspects. From the perspective of the mechanism used, gripping effectors are divided into:

- Screw mechanism

A screw mechanism consists of a shaft with a helical groove and a nut. Screw mechanisms convert rotary motion into linear motion or vice versa. There are two main groups of screw mechanisms, which are divided into sliding and rolling. Screw mechanisms are also often used in end effector designs. For gripping effects, a servo motor is used for rotational movement. Fig. 2 shows a model of an effector using a screw mechanism.

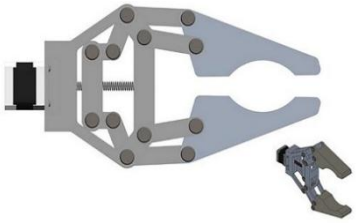

Figure 2. Effector with screw mechanism

- Rack and pinion effector

The rack and pinion mechanism belongs to the group of gear mechanisms. Gear mechanisms operate on the principle of meshing teeth. However, in the case of a rack transmission, the direction of movement changes from sliding to rotational, and vice versa. In Fig. 3, a diagram of an end effector with a double-acting piston for opening and closing the mechanism can be observed. A toothed rack is attached to the piston rod, which drives two toothed pinions. The pinions are firmly connected to the clamping parts and provide a relatively large clamping force.

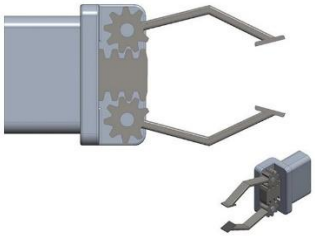

Figure 3. Effector with a comb mechanism

- Cam mechanism effector

Cam mechanisms are essentially bearings with enlarged outer raceways that are strong enough to be used as guide wheels. Effectors using a cam mechanism consist of a cam and a follower. These mechanisms convert rotary motion into linear motion. In Fig. 4 it is possible to observe the translational pair of a plane cam with a pulley. The mechanism also consists of pins and a spring. The sliding movement of the plane cam opens and closes the gripper jaws.

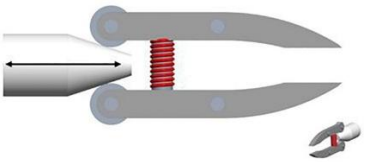

Figure 4. Cam mechanism effector

- Effector using a rope and pulley mechanism

In general, it can be said that pulley and rope mechanisms are evenly transmitting pulling mechanisms. These mechanisms can be designed to open and close mechanical types of grippers [Barnik 2018]. Since these are tensioning mechanisms, it is necessary to add a tensioning device to the structure. The tensioning device is intended to ensure proper tension of the rope and thus prevent movement of the rope on the pulley. The effector with a pulley and rope mechanism is shown in Fig. 5.

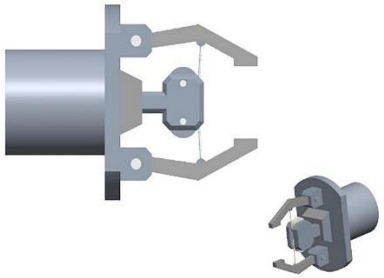

Figure 5. Roller gear effector

- Worm gear effectors

In this mechanism, all jaws of the gripping effector are controlled by a single worm gear. The servo drive is mounted on the base and drives a directly connected worm gear. The screw transfers the rotational motion to a set of wheels that are connected to each jaw of the effector. The screw mechanism also serves as a transmission. A model example of a gripping effector is shown in Fig. 6.

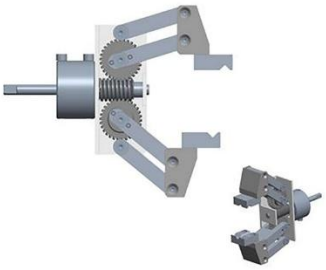

Figure 6. Effector with worm mechanism

2 MATERIALS AND METHODS

The CAD program PTC Creo was used to design a model of a gripping effector using the principles of "compliant" mechanisms. The advantage of using the Creo CAD program is the easy modification of the model throughout the entire production process. As mentioned in the introduction, the goal of "compliant" mechanisms is to reduce the number of mechanical parts needed to assemble the mechanism. In Fig. 7, it is possible to observe the designed model of the gripping

effector using a screw mechanism. The threaded rod is connected to the drive motor via a coupling. The individual parts are connected by a pin with one degree of freedom and can rotate relative to each other.

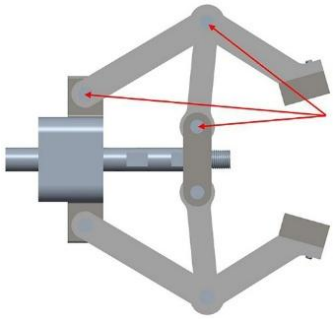

Figure 7. Proposed 3D model of the effector using a screw mechanism

When designing a "compliant" gripping effector, it was necessary to replace the pin with a bending member. The replacement of the pin with a bending member can be seen in Fig. 8 a). An alternative has been created for the gripping mechanism in which one bending member is omitted. The prototype with the bending member omitted can be seen in Fig. 8 b).

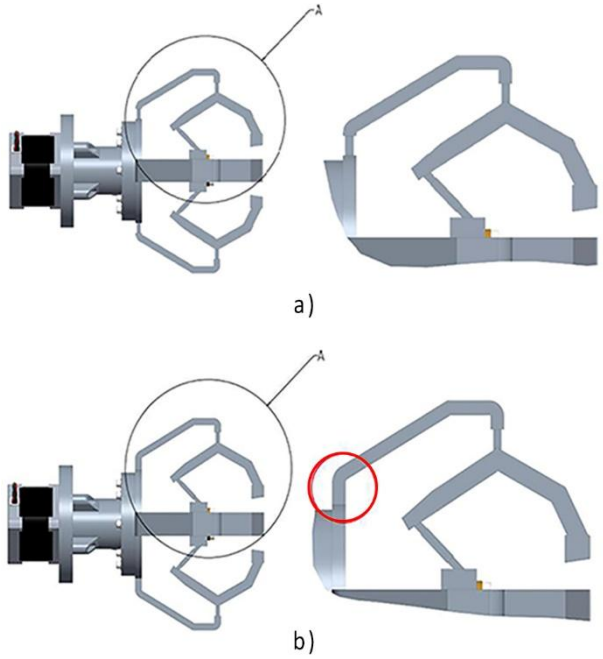

Figure 8. 3D model of the effector – a) Prototype A, b) Prototype B

The gripping effector consists of 11 components. The individual parts are connected using a detachable connection, so using a bolt and nut. This ensures easy replacement of the damaged part. The individual parts of the mechanism can be seen in Fig. 9.

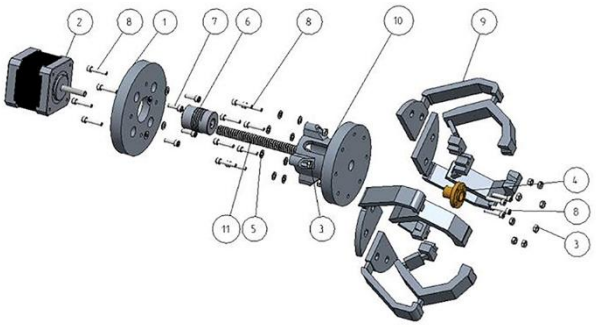

Figure 9. 3D model of the gripping effector assembly

The individual components of the gripping effector assembly are shown in Table 1.

Table 1. Gripper effector assembly components

No.	Component
1	Engine mount
2	Stepper motor Nema 17
3	Hexagon nut M3
4	Matrix T8
5	Flat washer M3
6	Flexible clutch
7	Screw M3x10
8	Screw M3x15
9	Grasping arm
10	Clamping flange
11	Threaded rod

Both prototypes of the gripping effector were manufactured using FDM additive technology. A self-made clone of the Prusa printer was used for production. The printer uses the marlin firmware, which is uploaded to the Arduino Mega 2560 programmable board with the RepRap module Ramps 1.4. Stepper motor control was provided using A4998 drivers. The "hot end" is from the E3D V6 model series. The maximum printing area is 250 x 250 x 200 mm. The Prusa slicer version 2.3.0 program was used to generate the G code. When designing the models, emphasis was placed on achieving the best possible printability and reducing the necessary supports (Fig. 10).

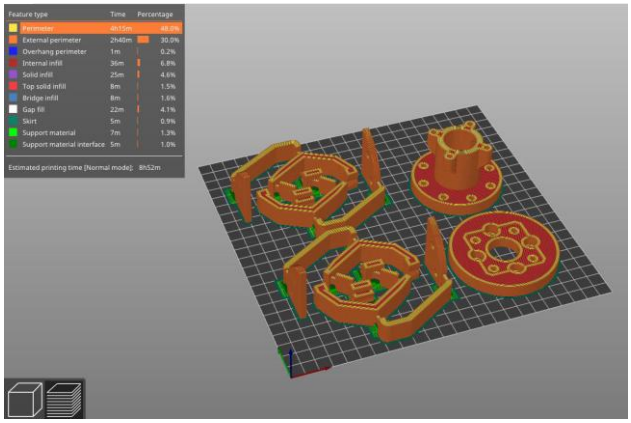

Figure 10. Layout of 3D models on the print bed

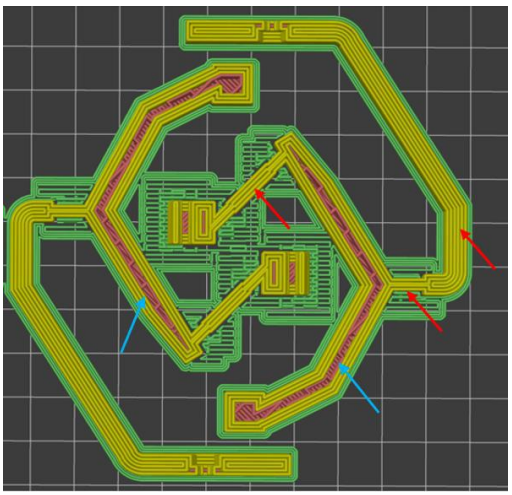

Figure 11. Parts printed with perimeter and parts printed with fill

To improve the bending properties, the bending members are pressed by the perimeter. By pushing the bending members through the perimeter, 100% parallelism of the layers was ensured. The other parts are printed with a fill density of 15% to save time. In Fig. 11, it is possible to observe the marked bending parts printed by the perimeter with a red arrow and the blue arrows indicate the parts printed with a fill density of 15%.
Fig. 12 shows individual models made from PLA material.

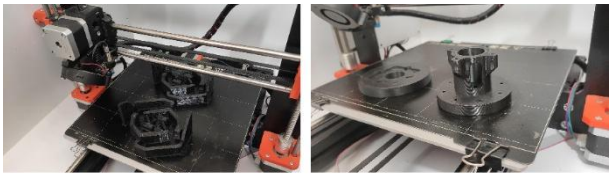

a) b)

Figure 12. Models made from PLA material - a) gripping arms, b) clamping flange and motor holder

For the greatest accuracy of the simulation in the Ansys software, it was necessary to measure the applied force. The measurement was performed using a universal membrane sensor EMS 20 from Emsyst in the range of 20N to 5kN. The measurement of the magnitude of the applied force for the gripping effector is shown in Fig. 13.

Figure 13. Measuring the magnitude of the applied force for a gripping effector

The measurement was repeated for both prototypes and for the PLA and PET-G materials from which the gripping effector was made. The magnitude of the force for individual gripping effector alternatives can be seen in Table 2.

Table 2. Results of force measurement

	Material	
	PLA	**PET-G**
Prototype A	142 N	95 N
Prototype B	163 N	105 N

For simulation purposes, the grasping effector model was simplified according to Fig. 14. In this image, the 3D model does not contain any bolts or nuts.

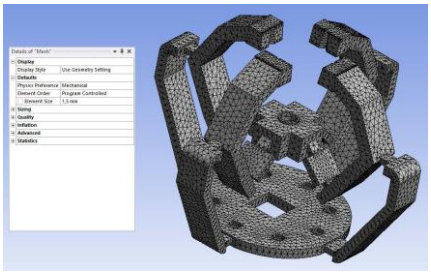

Figure 14. Meshed 3D model with element size 1.5 mm

For correct analysis results, the boundary conditions must be chosen to be identical to the boundary conditions of the real mechanism. To bind the gripping effector model, it was necessary to use two types of binding: "fixed support" and "displacement". The “fixed support” bond, which is shown in Fig. 15 a), was applied to the entire surface of the rear side of the effector. In fact, this part is fixed with screws to the clamping flange and has no degree of freedom. Another second bond is the “displacement” bond, which is shown in Fig. 15 b). This type of coupling allows movement in the selected axis. In the case of a gripping effector, there is the possibility of displacement in the x-axis.

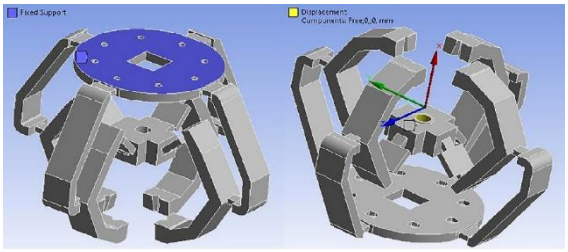

a) b)

Figure 15. Specifying a Fixed support constraint and a displacement constraint

After binding the 3D model, the next step was to determine the action and magnitude of the force. In Fig. 16, the area of application, direction and magnitude of the force can be seen. For each prototype, it was necessary to select the force, which was measured using a membrane sensor (Fig. 13). The individual measured force values were listed in Table 2.

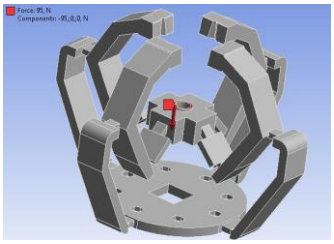

Figure 16. Defining force action

To control the stepper motor, an Arduino Uno development board, an easy driver, a joystick with output for two axes, a power supply, a capacitor, and a solderless dot array 830 were used. The connection diagram can be seen in Fig. 17 a). The Arduino IDE software version 1.8.19 was used to upload the program. At the beginning of the code, individual pins on the Arduino board were assigned with inputs and outputs to the drivers and joystick Fig. 17 b).

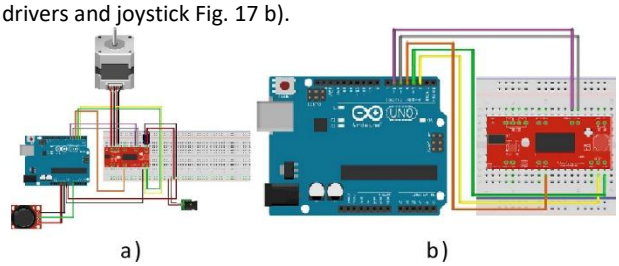

a) b)

Figure 17. a) Diagram of connecting the motor to the Arduino board, b) detail of connecting the Arduino pins and the "easy" driver

3 RESULTS AND DISCUSSION

A stress analysis and fatigue analysis were created for both gripper effector prototypes using Ansys software. The results of individual stresses for both prototypes and materials are shown in Fig. 18 and Fig. 19, with the 3D model of the effector with the applied stress shown on the left side of the image and the detail at the location of maximum stress shown on the right side of the image.

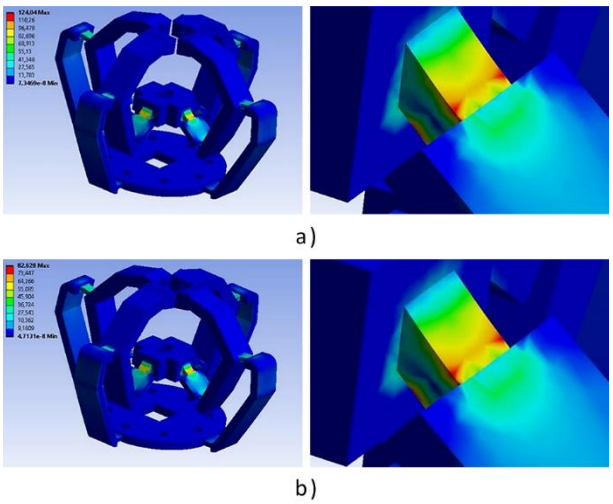

Figure 18. Stress analysis results for prototype A – a) PLA material, b) PET-G material

In Fig. 18, the results of the stress analysis for prototype A can be seen. The maximum stress for the PLA material was 124.04 MPa – Fig. 18 a) and the maximum stress for the PET-G material was 82.62 MPa – Fig. 18 b).

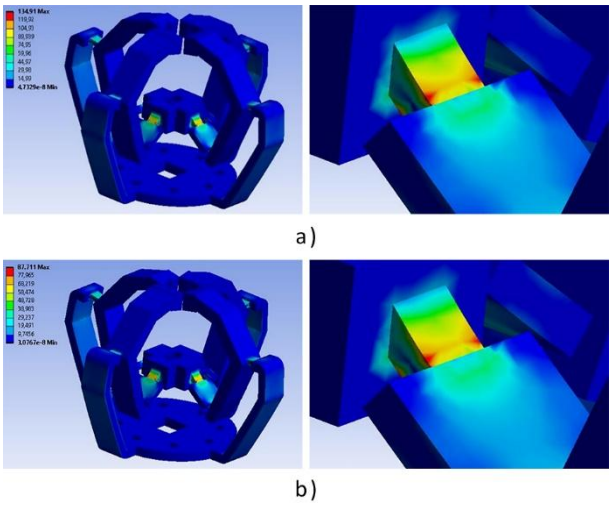

Figure 19. Stress analysis results for prototype B – a) PLA material, b) PET-G material

Fig. 19 shows the results of the stress analysis for prototype B. The maximum stress for the PLA material was 134.91 MPa – Fig. 19 a) and the maximum stress for the PET-G material was 87.71 MPa – Fig. 19 b). The stress analysis results showed that the PET-G material has lower stress generation levels than the PLA material.

The result of the fatigue analysis is a color scale that displays the number of cycles before fatigue failure of the material. The color scale with values can be seen in Fig. 20 and Fig. 21. Red areas are areas where material failure is expected. The places with the fewest cycles are identical to the places with the greatest stress.

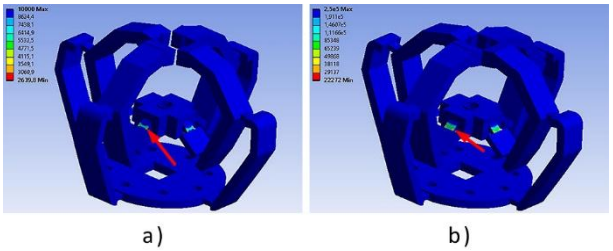

Figure 20. Results of fatigue stress analysis for prototype A – a) PLA material, b) PET-G material

Fig. 20 shows the results of the fatigue analysis for prototype A and Fig. 21 shows the results of the fatigue analysis for prototype B.

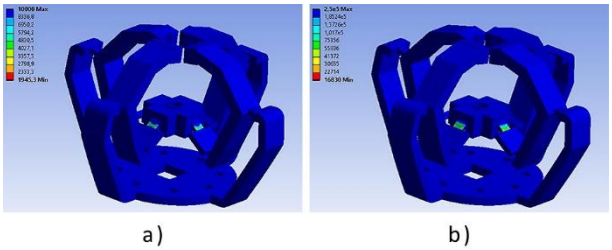

Figure 21. Results of fatigue stress analysis for prototype B – a) PLA material, b) PET-G material

Table 3. Summary of stress and fatigue analysis results

	Material	Acting force [N]	Tension [MPa]	Number of cycles
Prototype A	PET-G	95 N	82.62	22 272
Prototype B	PET-G	105 N	87.71	16 830
Prototype A	PLA	142	124.04	2639.8
Prototype B	PLA	163	134.91	1945.3

In Table 3, a comprehensive evaluation of the measurement and simulation results can be seen. If we evaluate the smallest required force, the smallest tension, and the largest number of cycles, prototype A made of PET-G material achieved the best results. Prototype B made of PLA material performed worst of the aforementioned criteria. The results also showed that if a smaller applied force is required, there is less stress generated in the mechanism, which has an impact on the number of cycles.

4 CONCLUSIONS

This article was devoted to the design of a "compliant" gripping effector. The design of the gripping effector model was designed in PTC Creo. An alternative prototype was subsequently designed for the gripping effector. The prototypes were subjected to measurements of the applied force required to close the mechanism's jaws and grasp an object. The magnitude of the force varied depending on the prototype and the type of material from which it was made. Subsequently, individual prototypes were subjected to analysis in the Ansys program. The analysis determined the magnitude of the stress and the location where the stress is concentrated. The results of the stress analysis can be linked to the results of force measurements, which showed that PLA requires a greater force to clamp the jaw of the gripping effector than PET-G. Thus, the reduction in the applied force, together with the different mechanical properties of the materials, resulted in a reduction in the generated stresses. It is also possible to say that the location at which the maximum voltage is generated does not change, only its magnitude changes. From the obtained stress data, simulation and analysis of material fatigue under cyclic loading was performed. The results of the fatigue analysis show that the PET-G material is more suitable in terms of cyclic material fatigue. The difference after rounding to whole completed cycles for prototype A made of PET-G and PLA was 19.632 cycles, which is approximately 8.5 times more. For prototype B, the difference after rounding was 14.885. Prototype B made of PET-G material can also complete approximately 8.5 times more cycles. The optimal variant was subsequently selected from the simulation results. In the last chapter, the work mapped the production, subsequent assembly of the mechanism, and its functioning using the Arduino programming board.

ACKNOWLEDGMENTS

The article was prepared with the support of the Ministry of Education, Research, Development, and Youth of the Slovak Republic through the KEGA grant No. 009TUKE-4/2024. It was also funded by the EU NextGenerationEU through the Recovery and Resilience Plan for Slovakia under the project No. 09I05-03-V02-00042.

REFERENCES

[Barnik 2018] Barnik, F., Vasko, M., Saga, M. Handrik, M., Sapietova, A. Mechanical properties of structures produced by 3D printing from composite materials. Matec Web Conf., 2018, Vol. 254, 01018. DOI: 10.1051/matecconf/201925401018.

[Elfferich 2022] Elfferich, J.F., Dodou, D., Santina, C. Della Soft Robotic Grippers for Crop Handling or Harvesting: A Review. IEEE Access, 2022, Vol. 10, pp. 75428-75443. DOI: 10.1109/ACCESS.2022.3190863.

[Kelemen 2022] Kelemen, M., et al. Robotic Gripper Actuated Using the Shape Memory Alloy Actuators. MM Sci. J., 2022, No. 3, pp. 5539-5545. DOI: 10.17973/MMSJ.2022_03_2022015.

[Li 2021] Li, S., Zhou, Y., Shan, Y., Chen, S., Han, J. Synthesis Method of Two Translational Compliant Mechanisms with Redundant Actuation. Mech. Sci., 2021, Vol. 12, pp. 983-995. DOI: 10.5194/ms-12-983-2021.

[Mykhailyshyn 2022a] Mykhailyshyn, R., Duchon, F., Mykhailyshyn, M., Majewicz Fey, A. Three-Dimensional Printing of Cylindrical Nozzle Elements of Bernoulli Gripping Devices for Industrial Robots. Robotics, 2022, Vol. 11. DOI: 10.3390/robotics11060140.

[Mykhailyshyn 2022b] Mykhailyshyn, R. and Xiao, J. Influence of Inlet Parameters on Power Characteristics of Bernoulli Gripping Devices for Industrial Robots. Appl. Sci., 2022, Vol. 12. DOI: 10.3390/app12147074.

[Mykhailyshyn 2023] Mykhailyshyn, R., Savkiv, V., Fey, A.M., Xiao, J. Gripping Device for Textile Materials. IEEE Trans. Autom. Sci. Eng., 2023, Vol. 20, pp. 2397-2408. DOI: 10.1109/TASE.2022.3208796.

[Sadeghian 2022] Sadeghian, R., Shahin, S., Sareh, S. Vision-Based Self-Adaptive Gripping in a Trimodal Robotic Sorting End-Effector. IEEE Robot. Autom. Lett., 2022. DOI: 10.1109/LRA.2022.3140793.

[Saga 2019] Saga, M., Vasko, M., Handrik, M., Kopas, P. Contribution to random vibration numerical simulation and optimisation of nonlinear mechanical systems. Sci. J. Silesian Univ. Technol. - series Transport, 2019, Vol. 103, pp. 143-154. DOI: 10.20858/sjsutst. 2019.103.11.

[Stojiljkovic 2023] Stojiljkovic, D., et al. Simulation, Analysis, and Experimentation of the Compliant Finger as a Part of Hand-Compliant Mechanism Development. Appl. Sci. 2023, Vol. 13. DOI: 10.3390/app13042490.

[Sun 2020] Sun, Y., Zhang, D., Liu, Y., Lueth, T.C. FEM-Based Mechanics Modeling of Bio-Inspired Compliant Mechanisms for Medical Applications. IEEE Trans. Med. Robot. Bionics, 2020, Vol. 2, pp. 364-373. DOI: 10.1109/TMRB.2020.3011291.

[Tkac 2022] Tkac, J., Pollak, M. Design and Analysis of a Bending Mechanism Produced By Fdm Technology. MM Sci. J. 2022, Vol. June, pp. 5614-5619. DOI: 10.17973/MMSJ.2022_06_2022018.

[Vishnu 2022] Vishnu,R., Parsa, S., Parsons, S., Galamzan, A.E. Peduncle Gripping and Cutting Force for Strawberry Harvesting Robotic End-Effector Design. In: Proc. 4th Int. Conf. on Control and Robotics (ICCR 2022), Guangzhou, China, 2022, pp. 59-64. DOI: 10.1109/ICCR55715.2022.10053882.

[Wang 2024] Wang, F., Fan, Y. Structural Design and Analysis of a Picking Robot Arm Using Parallel Grippers. Adv. Mech. Eng., 2024, Vol. 16. DOI: 10.1177/16878132241304610.

[Zhang 2020] Zhang, B., Xie, Y., Zhou, J., Wang, K., Zhang, Z. State-of-the-Art Robotic Grippers, Grasping and Control Strategies, as Well as Their Applications in Agricultural Robots: A Review. Comput. Electron. Agric., 2020, Vol. 177, 105694. DOI: 10.1016/J.COMPAG.2020.105694.

CONTACTS:

Jozef Tkac, Ing. PhD.
Technical University of Kosice
Faculty of Manufacturing Technologies with a seat in Presov
Department of Computer Aided Manufacturing Technologies
Sturova 31, Presov, 080 01, Slovak Republic
+421 55 602 6364, jozef.tkac@tuke.sk